Asian Journal of Chemistry; Vol. 31, No. 8 (2019), 1805-1808

ASIAN JOURNAL OF CHEMISTRY

https://doi.org/10.14233/ajchem.2019.22054

Optical, Structural and Gas Sensing Studies on Tin Oxide Thin Films

RAJESH KUMAR* and SWATI CHAWLA

Department of Physics, Lovely Professional University, Phagwara-144411, India

*Corresponding author: E-mail: rajesh.12236@lpu.co.in

Received: 7 March 2019; *Accepted*: 12 April 2019; *Published online*: 28 June 2019; AJC-19456

In this paper, pure and copper doped tin oxide thin films were grown on glass substrates by thermal evaporation technique for gas sensing applications. Optical, structural and gas sensing properties were investigated for their application for gas sensing applications. The thickness of the samples was kept about 300 nm. The films were annealed at 400 ºC for 4 h in the presence of air. The gas sensing studies were carried out for hydrogen sulphide and ethanol gas. The sensitivity was quite high for hydrogen sulphide gas but little sensitivity towards hydrocarbon gases.

Keywords: Thermal evaporation, Tin oxide, Gas sensitivity.

INTRODUCTION

The environmental pollution is the major problem of the world for last many decades. The gases emitted by the industrial units, vehicular traffic, volcanic eruptions, floods and salt mines are the major contributors of the environmental pollution. Out of all the gases being emitted by these sources, hydrogen sulphide and liquefied petroleum gas (LPG) are the major pollutants of the atmosphere. Hydrogen sulphide is present wherever there is vegetative stink and stagnation and accumulation of water *i.e.* in swamps and oil fields [1]. On the other hand, liquefied petroleum gas is used widely in the household kitchens. Human nose detects 0.02 ppm of H_2S in air but proves fatal when inhaled continuously for longer duration of time. Similarly, accidental leakage of LPG and other hydrocarbon gases can result in the formation of explosive mixture with air. Therefore, there is an urgent need to detect these gases in parts per billion (ppb) levels in air for the safety of environment. Due to the use of semiconductor materials for gas sensor applications, the detection and monitoring of hazardous gases has become easier over the other technologies like gas layer chromatography (GLC) and FTIR spectroscopy.

With respect to gas sensors, tin oxide is a wonderful material as its properties can be varied to suit the gas sensing applications. It is well known that the non-stoichiometric tin oxide is an n-type semiconductor with a wide band gap of 3.6 eV [2,3]. Tin oxide has high electrical conductivity due to the presence of high concentration of oxygen vacancies. The conductivity of tin oxide also depends upon the type of gases present in the atmosphere. Owing to these properties, tin oxide thin films find applications in the fabrication of transistors, transparent conducting electrodes for solar cells, protective coatings on glassware in LCDs, LEDs, gas sensing materials and infrared reflectors for glass windows, *etc*. [4-10]. It is worth to report that a variety of gases like CO, NOx, hydrogen sulphide, H_2, methane, compressed natural gas (CNG) and liquefied petroleum gas (LPG) have been tested for gas sensing applications on tin oxide semiconducting materials [11-13].

Various techniques have been employed to deposit thin films of tin oxide, both in doped and undoped form. These methods include thermal evaporation, chemical vapour deposition, magnetron sputtering, laser ablation, spray pyrolysis and sol gel and technology related to the deposition of thick films [14-21]. It has been observed by various researchers that the response to a gaseous environment by a sensor depends upon stoichiometry of the material, size of the grains, structure of thin film surface *i.e.* whether it is porous or not, number of imperfections on the film surface, film thickness and temperature at which the film is being tested for response. It has been further reported that thin films of tin oxide show faster and higher response towards the gaseous ambient than the thick films. This is probably due to the fact that gas molecules interact well with the thin

film surface as compared to the thick film surface [22-25]. Thick films of SnO_2 doped with 5 % CuO were found to have very high sensitivity of nearly 35000 for 50 ppm of hydrogen sulphide in air at an operating temperature of 200 ºC. The sensitivity of the gas sensor is given by

$$S = \frac{R_a}{R_g} \quad (1)$$

The films demonstrated recovery like a switch in 1 min with a response time of 15 min [26,27]. In this paper, we describe the deposition and optical, structural and gas sensing properties of tin oxide thin films both in pure and doped form by simple and cost effective technique such as thermal evaporation.

EXPERIMENTAL

The glass substrates were cleaned before deposition with liquid soap, acetone and followed by ultrasonic cleaner to ensure the removal of any kind of impurities (organic or inorganic). The deposition of thin films was performed in a vacuum coating unit fabricated by HINDHIVAC (Bangalore) India. The deposition chamber of the coating unit was evacuated to a base pressure of 1.5×10^{-5} mbar. The glass substrates were heated resistively at 60 ºC during deposition as the film adheres very well with the heated substrates. The source to substrate distance was kept at about 20 cm. A tin piece and a copper piece were evaporated simultaneously in a molybdenum boat. Two types of films were deposited, one having 3.5 % copper and other 5 % copper as a dopant by weight. During deposition, the current passing through the boat was about 50-60 amperes, deposition time was kept 16-18 min with a deposition rate of 3.0-3.5 Å/s. The thickness of both the types of films was determined by quartz crystal monitor and kept at 300 nm.

RESULTS AND DISCUSSION

Optical characteristics: Figs. 1 showed the wavelength *versus* absorption characteristics of 3.5 % copper doped and 5 % copper doped SnO_2 thin films. In Fig. 1(a), maximum absorption occured at a wavelength of 373 nm while in Fig. 1(b) maximum absorption occured at 296 nm. The absorption values are constant in the visible range. The decrease in maximum absorption value with increasing copper content is due to increase in the density of copper atoms in tin oxide matrix.

The absorption coefficient of thin films was determined from the following formula:

$$\alpha = \frac{2.303A}{t} \quad (2)$$

Fig. 2 shows the direct band gaps of pure and 3.5-5 % Cu-doped thin films. It has been found that band gap of all the types of films lie between 3-4 eV which is in agreement with the literature [28-30]. The copper doping appears to have no effect on the direct band gap which is in accordance with as reported in the literature [31].

Structural characteristics: The structural characteristics of thin films were determined with X-ray diffraction technique. Fig. 3 showed the X-ray diffractograms for thin films of pure tin oxide, tin oxide thin films doped with 3.5 % Cu and tin oxide thin films doped with 5 % Cu. XRD measurements were carried out using X'PERT-PRO diffractometer (PAN-Analytical, United Kingdom) with CuKα wavelength of 1.54 Å. The diffraction patterns were measured in the diffraction angle range of 0-80º for all the samples. The appearance of well defined peaks at almost similar angles of 2θ indicates the presence of crystalline rutile structure [32]. Various peaks were observed in the diffractographs, namely 210(022), 250(110), 300(020), 320 (101),

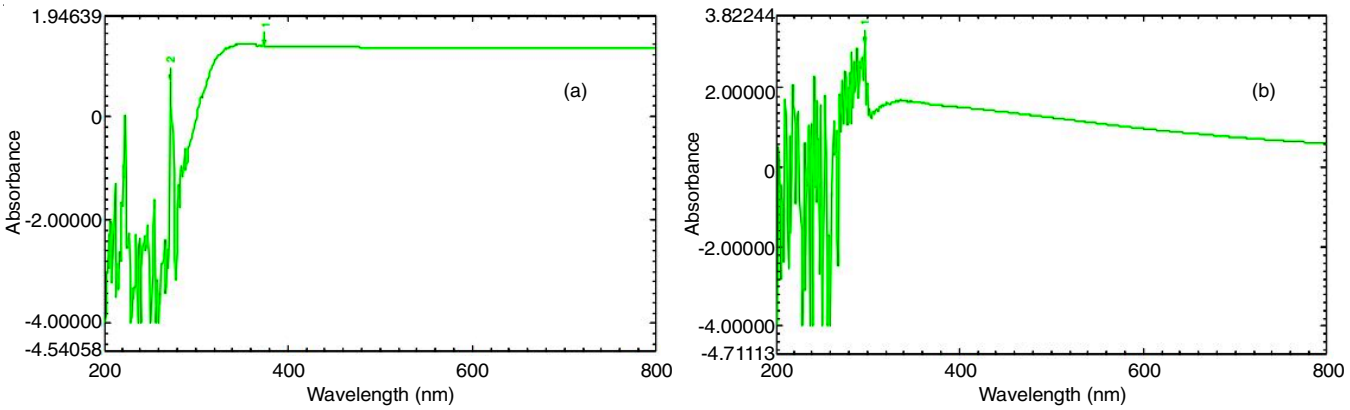

Fig. 1. Variation of absorption with increasing wavelength for 3.5 % Cu doped SnO_2 (a) and 5 % Cu doped SnO_2 (b)

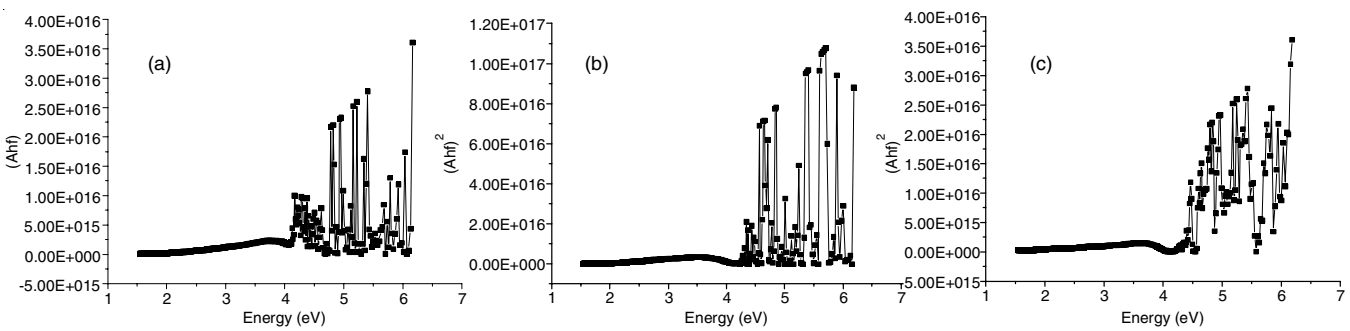

Fig. 2. Direct band gaps of pure tin (a); 5 % Cu doped SnO_2 (b) and 3.5 % Cu doped SnO_2 (c)

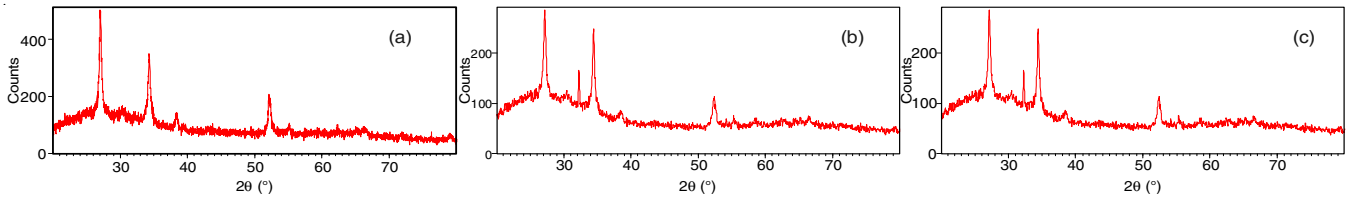

Fig. 3. X-ray diffractograms of pure tin (a); 3.5 % Cu doped SnO_2 (b) and 5 % Cu doped SnO_2 (c)

340(101), 380(200) and 520(211). The peaks at 210, 320 appeared specifically in the diffraction patterns of Cu-doped SnO_2 thin films. This data corresponds well with Joint Committee on Powder Diffraction Standards (JCPDS) card no. 88-0287. The sharpness and well defined nature of diffraction peaks indicate that the thin films are highly crystalline in nature. From all the diffractographs, it has been observed that the peak intensity is highest for the peak appearing at an angle of 21°. This points to the fact that Sn atoms preferred the (022) plane and formed a rutile structure making bonds with oxygen atoms. Present films showed negligible reflectance indicating that the films grown by technique are of high purity. The grain size of thin films was calculated using Debye-Scherrer equation:

$$D = \frac{k\lambda}{\beta \cos\theta} \qquad (3)$$

where "k" is called shape factor whose value lies between 0.8-1.39 (usually taken as 0.94), λ is the wavelength of radiation, β is called FWHM (Full width at half maximum) in radians, θ is the position of maximum of diffraction [32]. From the above formula, the size of the grains was found to be a few nanometers which make these films suitable for gas sensing applications.

Gas sensing characteristics: The gas sensing characteristics of thin films were measured by an indigenously made two probe set up made in a dessicator having volume of nearly 11 L.

The hydrogen sulphide with various concentrations was injected with ordinary syringes into the dessicator. The changes in the current and hence corresponding changes in resistance through thin film elements was continuously monitored by an auto-ranging digital pico-ammeter (Keithley Make, USA). Fig. 4 shows the sensor signal as a function of gas concentration at three operating temperatures. The signal falls with increasing temperature and was as high as 3.6×10^5 at 160 ºC for 50 ppm of H_2S. The 80 % response time at this operating temperature was about 10 min and on the removal of gas, time, T_{100}, taken for the sensor signal to fall to 1/100th of its value in the presence of H_2S gas was ~ 3 min.

Fig. 5 shows the typical response and recovery plots for 50 ppm H_2S gas at three operating temperatures. It is clear from that both the response and recovery times improve with increase in operating temperature. At 200 ºC, 80 % response time for the sensor element was only 4 min and T_{100} was about 1 min. The 100 % recovery time at 160 ºC was nearly 84 min, while it decreased to only 18 min at 200 ºC. An H_2S sensor should be able to detect a few ppm levels of H_2S gas with high sensitivity. It is, therefore, important to measure the sensor characteristics at very low (< 10 ppm) H_2S concentrations. This CuO SnO_2 thin film element has an H_2S signal of about 600 for 5 ppm H_2S at 160 ºC. The 80 % response time was 6 min and on the

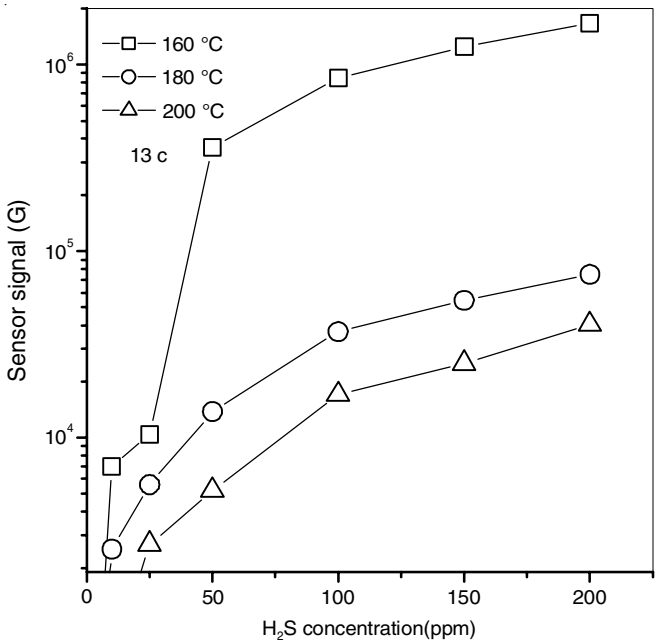

Fig. 4. Variation of H_2S sensor signal with gas concentration at different operating temperatures

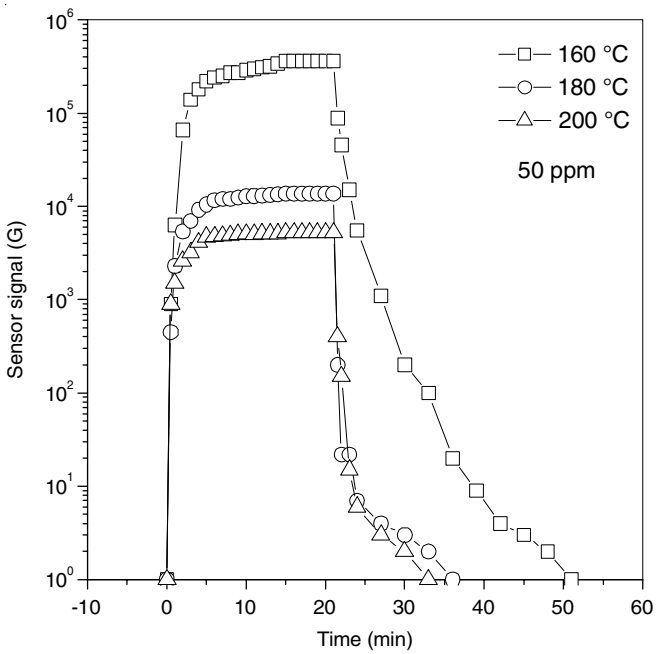

Fig. 5. Typical sensor response and recovery transients for 50 ppm of H_2S at three different operating temperatures

removal of gas, time, T_{100}, was about 19 min, while the 100 % recovery time at this temperature was nearly 74 min.

Mechanism of gas sensing: It is well known that non-stoichiometric SnO_2 is an n-type semiconductor while CuO is

a p-type semiconductor. They form p-n junctions having high resistance. The high sensitivity of Cu-doped thin films towards hydrogen sulphide gas is based on the metal like conductivity of CuS on exposure to hydrogen sulphide according to the following chemical reaction:

$$CuO + H_2S \longrightarrow CuS + H_2O \quad (4)$$

The p-n junctions are ruptured on exposure to H_2S leading to the formation of CuS and resulting in decrease of electrical resistance. During recovery, CuS is converted back to CuO on exposure to ambient air according to the following reaction [26,33]:

$$2CuS + 3O_2 \longrightarrow 2CuO + 2SO_2 \quad (5)$$

Present SnO_2 thin films did not show any response towards even 1000 ppm of ethanol gas. The mechanism to explain the decrease in the resistance of pure SnO_2 thin films on exposure to H_2S gas was suggested by Capehart and Chang [34]. The little sensitivity towards hydrogen sulphide of pure SnO_2 is explained as follows. As mentioned above, non-stoichiometric SnO_{2-x} is an n-type semiconductor. On exposure to H_2S, the following reversible reaction is believed to take place on the surface of SnO_{2-x} species (eqn. 6)

$$SnO_{2-x} + \Delta H_2S \rightleftharpoons SnO_{2-x-3\Delta} + \Delta H_2O + \Delta SO_2 + 6\Delta e^- \quad (6)$$

Conclusion

The fabrication of gas sensor for hydrogen sulphide is developed using pure and copper doped tin oxide thin films prepared by a simple method of thermal evaporation. It is concluded that the films had particle size of a few nanometers and sensing action depends upon the breakage of SnO_2-CuO pn junctions on exposure to hydrogen sulphide gas. The films were quite selective to hydrogen sulphide and virtually no sensitivity towards ethanol and LPG gases.

ACKNOWLEDGEMENTS

The authors sincerely thank the cooperation extended by Mr. Jagtar Singh of Sophisticated Analytical Instrumentation Facility (SAIF), Panjab University, Chandigarh, India for X-ray diffraction studies.

CONFLICT OF INTEREST

The authors declare that there is no conflict of interests regarding the publication of this article.

REFERENCES

1. B. Elvers, S. Hawkins and G. Schulz, Ullmann Encyclopedia of Industrial Chemistry, VCH: Weinheim, vol. A13, p. 467 (1989).
2. L.D. Loch, *J. Electrochem. Soc.*, **110**, 1081 (1963); https://doi.org/10.1149/1.2425588.
3. C. Kilic and A. Zunger, *Phys. Rev. Lett.*, **88**, 095501 (2002); https://doi.org/10.1103/PhysRevLett.88.095501.
4. M.S. Arnold, P. Avouris, Z.W. Pan and Z.L. Wang, *J. Phys. Chem. B*, **107**, 659 (2003); https://doi.org/10.1021/jp0271054.
5. A.M. Gheidari, E.A. Soleimani, M. Mansorhoseini, S. Mohajerzadeh, N. Madani and W. Shams-Kolahi, *Mater. Res. Bull.*, **40**, 1303 (2005); https://doi.org/10.1016/j.materresbull.2005.04.007.
6. M. Nakagawa, T. Amano and S. Yokokura, *J. Non-Cryst. Solids*, **218**, 100 (1997); https://doi.org/10.1016/S0022-3093(97)00238-X.
7. U. Betz, M. Kharrazi Olsson, J. Marthy, M.F. Escolá and F. Atamny, *Surf. Coat. Technol.*, **200**, 5751 (2006); https://doi.org/10.1016/j.surfcoat.2005.08.144.
8. N. Butta, L. Cinquegrani, E. Mugno, A. Tagliente and S. Pizzini, *Sens. Actuators B Chem.*, **6**, 253 (1992); https://doi.org/10.1016/0925-4005(92)80064-5.
9. A. Keshavaraja, B.S. Jayashri, A.V. Ramaswamy and K. Vijayamohanan, *Sens. Actuators B Chem.*, **23**, 75 (1995); https://doi.org/10.1016/0925-4005(94)01528-P.
10. G.H. Lindner, Non-iridescent, Haze-free Infrared Reflecting Coated Glass Structures, U.S. Patent 4737388 (1988).
11. O.K. Varghese and L.K. Malhotra, *Sens. Actuators B Chem.*, **53**, 19 (1998); https://doi.org/10.1016/S0925-4005(98)00288-3.
12. N.S. Baik, G. Sakai, N. Miura and N. Yamazoe, *Sens. Actuators B Chem.*, **63**, 74 (2000); https://doi.org/10.1016/S0925-4005(99)00513-4.
13. R.S. Niranjan and I.S. Mulla, *Mater. Sci. Eng. B*, **103**, 103 (2003); https://doi.org/10.1016/S0921-5107(03)00154-5.
14. E. Comini, G. Faglia, G. Sberveglieri, Z. Pan and Z.L. Wang, *Appl. Phys. Lett.*, **81**, 1869 (2002); https://doi.org/10.1063/1.1504867.
15. V.S. Vaishnav, P.D. Patel and N.G. Patel, *Thin Solid Films*, **490**, 94 (2005); https://doi.org/10.1016/j.tsf.2005.04.006.
16. P.M. Gorley, V.V. Khomyak, S.V. Bilichuk, I.G. Orletsky, P.P. Horley and V.O. Grechko, *Mater. Sci. Eng.*, **118**, 160 (2005); https://doi.org/10.1016/j.mseb.2004.12.026.
17. J. Jeorg, S.P. Choi, K.J. Hong, H.J. Song and J.S. Park, *J. Korean Phys. Soc.*, **48**, 960 (2006).
18. C.K. Kim, S.M. Choi, H. Noh, J.H. Lee, C. Hong, H.B. Chae, G.E. Jang and H.D. Park, *Sens. Actuators B Chem.*, **77**, 463 (2001); https://doi.org/10.1016/S0925-4005(01)00726-2.
19. H. Pirmoradi, J. Malakootikhah, M. Karimipour, A. Ahmadpour, N. Shahtahmasebi and F.E. Koshky, *Middle East J. Sci. Res.*, **8**, 253 (2011).
20. O. Culha, M.F. Ebeoglugil, I. Birlik, E. Celik and M. Toparli, *J. Sol-Gel Sci. Technol.*, **51**, 32 (2009); https://doi.org/10.1007/s10971-009-1956-8.
21. V. Guidi, M.A. Butturi, M.C. Carotta, B. Cavicchi, M. Ferroni, C. Malagu, G. Martinelli, D. Vincenzi, M. Sacerdoti and M. Zen, *Sens. Actuators B Chem.*, **84**, 72 (2002); https://doi.org/10.1016/S0925-4005(01)01077-2.
22. D.S. Vlachos, C.A. Papadopoulos and J.N. Avaritsiotis, *J. Appl. Phys.*, **80**, 6050 (1996); https://doi.org/10.1063/1.363562.
23. C. Xu, J. Tamaki, N. Miura and N. Yamazoe, *Sens. Actuators B Chem.*, **3**, 147 (1991); https://doi.org/10.1016/0925-4005(91)80207-Z.
24. T. Becker, S. Ahlers, C. Bosch-v.Braunmühl, G. Müller and O. Kiesewetter, *Sens. Actuators B Chem.*, **77**, 55 (2001); https://doi.org/10.1016/S0925-4005(01)00672-4.
25. F. Hossein-Babaei and M. Orvatinia, *Sens. Actuators B Chem.*, **89**, 256 (2003); https://doi.org/10.1016/S0925-4005(02)00472-0.
26. J. Tamaki, T. Maekawa, N. Miura and N. Yamazoe, *Sens. Actuators B Chem.*, **9**, 197 (1992); https://doi.org/10.1016/0925-4005(92)80216-K.
27. D.J. Yoo, J. Tamaki, S.J. Park, NorioMiura and N. Yamazoe, *Jpn. J. Appl. Phys.*, **34(Part 2, No. 4A)**, L455 (1995); https://doi.org/10.1143/JJAP.34.L455.
28. S.-C. Lee, J.-H. Lee, T.-S. Oh and Y.-H. Kim, *Sol. Energy Mater. Sol. Cells*, **75**, 481 (2003); https://doi.org/10.1016/S0927-0248(02)00201-5.
29. S.K. Tripathy, B.P. Hota and P.V. Rajeswari, *Bull. Mater. Sci.*, **36**, 1231 (2013); https://doi.org/10.1007/s12034-013-0582-9.
30. J.O. Ajayi and D.B. Agunbiade, *Int. J. Res. Appl. Sci. Eng. Technol.*, **3**, 821 (2015).
31. P.G.L. Baker, R.D. Sanderson and A.M. Crouch, *Thin Solid Films*, **515**, 6691 (2007); https://doi.org/10.1016/j.tsf.2007.01.042.
32. T. Pradeep, A Textbook of Nanoscience and Nanotechnology, McGraw Hill Education, 4th Reprint (2012).
33. T. Maekawa, J. Tamaki, N. Miura and N. Yamazoe, *J. Mater. Chem.*, **4**, 1259 (1994); https://doi.org/10.1039/JM9940401259.
34. T.W. Capehart and S.C. Chang, *J. Vac. Sci. Technol.*, **18**, 393 (1981); https://doi.org/10.1116/1.570794.